Received: 7 August 2021 | Revised: 4 November 2021 | Accepted: 8 December 2021

DOI: 10.1002/jsp2.1187

RESEARCH ARTICLE

JOR Spine OPEN ACCESS

Injectable decellularized nucleus pulposus tissue exhibits neuroinhibitory properties

Logan M. Piening[1] | David J. Lillyman[1] | Fei San Lee[1] | Alvaro Moreno Lozano[1] | Jeremy R. Miles[2] | Rebecca A. Wachs[1]

[1]Biological Systems Engineering Department, University of Nebraska-Lincoln, Lincoln, Nebraska, USA

[2]USDA, ARS, US Meat Animal Research Center, Clay Center, Nebraska, USA

Correspondence
Rebecca A. Wachs, Biological Systems Engineering Department, University of Nebraska-Lincoln, P.O. Box 830726, Lincoln, Nebraska, 68583-0726
Email: rebecca.wachs@unl.edu

Funding information
National Science Foundation

Abstract

Background: Chronic low back pain (LBP) is a leading cause of disability, but treatments for LBP are limited. Degeneration of the intervertebral disc due to loss of neuroinhibitory sulfated glycosaminoglycans (sGAGs) allows nerves from dorsal root ganglia to grow into the core of the disc. Treatment with a decellularized tissue hydrogel that contains sGAGs may inhibit nerve growth and prevent disc-associated LBP.

Methods: A protocol to decellularize porcine nucleus pulposus (NP) was adapted from previous methods. DNA, sGAG, α-gal antigen, and collagen content were analyzed before and after decellularization. The decellularized tissue was then enzymatically modified to be injectable and form a gel at 37°C. Following this, the mechanical properties, microstructure, cytotoxicity, and neuroinhibitory properties were analyzed.

Results: The decellularization process removed 99% of DNA and maintained 74% of sGAGs and 154% of collagen compared to the controls NPs. Rheology demonstrated that regelled NP exhibited properties similar to but slightly lower than collagen-matched controls. Culture of NP cells in the regelled NP demonstrated an increase in metabolic activity and DNA content over 7 days. The collagen content of the regelled NP stayed relatively constant over 7 days. Analysis of the neuroinhibitory properties demonstrated regelled NP significantly inhibited neuronal growth compared to collagen controls.

Conclusions: The decellularization process developed here for porcine NP tissue was able to remove the antigenic material while maintaining the sGAG and collagen. This decellularized tissue was then able to be modified into a thermally forming gel that maintained the viability of cells and demonstrated robust neuroinhibitory properties

in vitro. This biomaterial holds promise as an NP supplement to prevent nerve growth into the native disc and NP in vivo.

KEYWORDS
biomaterials, degeneration, extracellular matrix, regenerative medicine

1 | INTRODUCTION

Low back pain (LBP) affects four out of five people in the world at least once in their lifetime, with 20% of those affected developing *chronic* LBP.[1,2] The high incidence of chronic LBP has made it the leading cause of years lived with disability for the past three decades.[3] One common type of chronic LBP is discogenic pain. Discogenic pain patients exhibit nerve growth deep within the previously aneural disc.[4,5] These nerve fibers are stimulated and sensitized by the catabolic disc environment.[6,7] The current gold standard of treatment for end-stage chronic LBP patients is a spinal fusion, which can be invasive, have high complication rates (14.3%[8]-16%[9] of patients), high costs,[8-10] long recovery times,[11] and lead to reduced range of motion and increased potential for adjacent level degeneration.[12,13] An alternative low-risk treatment that focuses on reducing a patient's pain holds great potential for the treatment of LBP.

The intervertebral disc is composed of a gelatinous nucleus pulposus (NP) core surrounded by a lamellar annulus fibrosus (AF).[14] The healthy disc is predominantly avascular and aneural and receives the majority of nutrients from diffusion through adjacent cartilaginous end plates.[14,15] Aging and injury can trigger disc degeneration, resulting in thickening of the end plates, reducing diffusion of nutrients into the NP.[16-18] This reduction in nutrient diffusion can lead to NP cell senescence.[19] Senescent NP cells secrete inflammatory cytokines and degradative enzymes, creating a catabolic environment that breaks down matrix components such as aggrecan.[20-22] Intact aggrecan has neuroinhibitory properties due to sulfated glycosaminoglycan (sGAG) side chains and thus naturally inhibits nerve growth into a healthy disc.[23] During degeneration, cleavage of these sGAG side chains reduces the neuroinhibitory properties of the disc.[24-27] Further, senescent NP cells secrete several molecules that increase nerve growth, such as nerve growth factor (NGF) and brain-derived neurotrophic factor (BDNF).[7,28,29] The loss of potently neuroinhibitory sGAGs and increased expression of NGF and BDNF result in ideal conditions for the ingrowth of nerve fibers into degenerated discs. Once painful nerve fibers are present in the disc, they can be sensitized and stimulated by the harsh catabolic environment of the degenerating disc, leading to pain.[30] A treatment that restores neuroinhibitory sGAGs to the degenerate painful disc has the potential to prevent disease progression by preventing nerve growth. Decellularized tissue scaffolds fabricated from healthy NP tissue hold promise to restore sGAGs and reintroduce neuroinhibitory properties to the NP and prevent pain progression.

Decellularized tissue has been widely used over the past 50 years to engineer tissues such as urinary bladder matrix,[31] dermis,[32,33] and small intestinal submucosa.[34-36] Decellularized tissues have been successful in treatments because decellularized scaffolds have similar properties, compositions, and architecture to native tissue, thereby improving their function and cellular recognition in vivo.[37] For decellularization of the NP, maintenance of the extracellular matrix proteins and proteoglycans is crucial for its eventual function in the disc. Several groups have developed decellularization methods for the NP by using various detergents of differing concentrations and incubation times.[38-44] These decellularization methods focus on improving the removal of cellular materials and on maintaining native proteins such as sGAGs.[2,38-44] However, to date, no group has investigated the neuroinhibitory properties of decellularized NP from the maintenance of native sGAGs, which could play a crucial role in preventing LBP. Therefore, the goal of this paper is to develop a decellularization method that removes cells and maintains sGAGs from porcine NP and investigate the neuroinhibitory properties of the decellularized NP scaffold.

In this paper, we developed a decellularization method for intact porcine NP, adapted from our previous methods.[2] The decellularized NP was characterized to determine the removal of DNA and the maintenance of sGAG and collagen and then modified into a thermally forming gel (regelled NP) (Figure 1). The cytotoxicity and neuroinhibitory properties of the regelled NP were tested using primary sensory neurons in a previously developed culture model from our lab.[45] The regelled NP created a suitable environment for NP cells to grow and remodel the matrix while inhibiting nerve growth. These results suggest that a decellularized NP gel could be used as supplemental treatment to prevent nerve growth in a degenerated disc and prevent pain progression.

2 | MATERIALS AND METHODS

2.1 | Validation of whole disc decellularization methods

2.1.1 | Whole disc decellularization

Cervical spines from commercial line Landrace/Yorkshire/Duroc young female pigs (~200 days of age) were aseptically collected and frozen (−80°C) following humane slaughter at the US Meat Animal Research Center Abattoir (Clay Center, Nebraska; USDA Material Transfer Agreement). Intact spines were thawed for 2 days at 4°C. The spines were then cleaned aseptically, and the NPs of the C2-C7 intervertebral discs were surgically removed. Control NPs from each

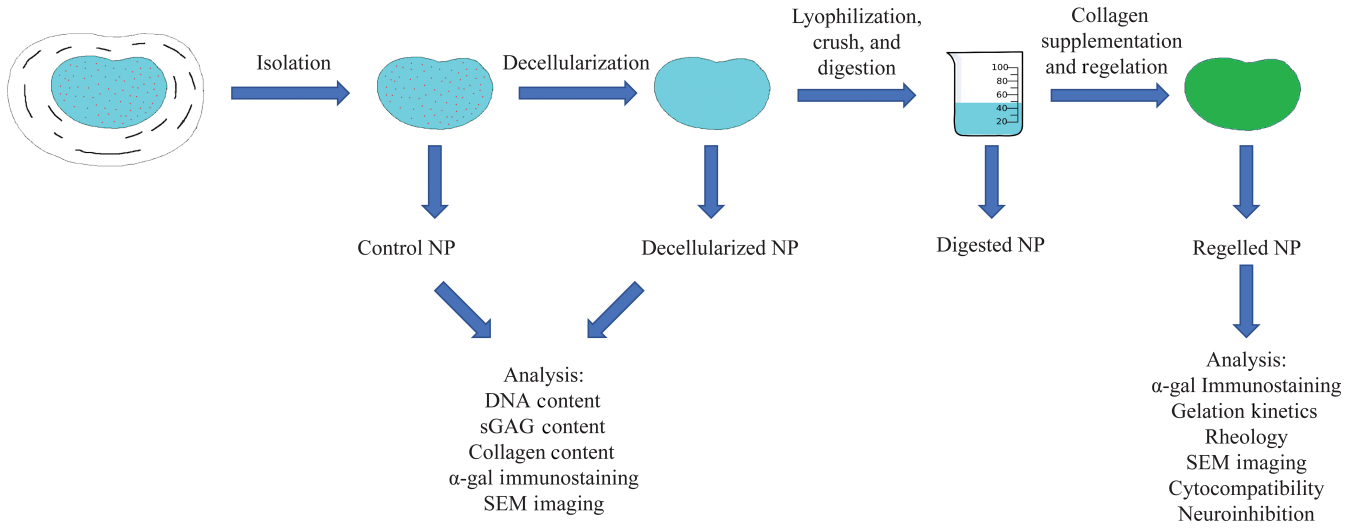

FIGURE 1 Schematic illustration of the porcine nucleus pulposus decellularization, digestion, and regelation process and parallel analyses. SEM, Scanning electron microscopy; NP, nucleus pulposus

spine were either (1) fixed in 4% paraformaldehyde (PFA) for 30 minutes, followed by 3 × 15-minute washes in 1× phosphate-buffered saline (PBS) for imaging, (2) eluted in media for cytotoxicity studies, or (3) frozen at −80°C and lyophilized for 2 days (FreeZone 4.5 L Freeze Dryer [7750020, Labconco]) for additional analyses described below. Remaining NPs were decellularized following the process as outlined in Table 1. This procedure was adapted from Wachs et al.[2] by processing each whole intact NP at room temperature in a 50-ml tube (89 039, VWR) filled up to the 45-ml mark, spinning on an orbital shaker (EW-07650, Stuart) at 18 rpm. Changes made to the previous protocol include replacing Triton X-200 (discontinued) with sodium deoxylcholate (Sigma-Aldrich), excluding RNase digestion, altering times for detergent washes, and including 1× PBS and water washes at the end of the process. Decellularized NPs were processed as outlined above with either fixation, elution, or lyophilization. A minimum of three spines were used for each analysis to account for animal variability. To account for increased variability in decellularized NP samples compared to control NP samples, at least one unprocessed control NP and at least one decellularized NP were analyzed for each spine, for a total of at least three control NPs and decellularized NPs.

2.1.2 | DNA content

DNA content of control and decellularized NP samples was analyzed using the Quant-iT PicoGreen dsDNA Assay Kit (P7589, Thermo Fisher) according to the manufacturer's instructions to verify the removal of antigenic DNA remnants after decellularization. Briefly, lyophilized control and decellularized NP samples were digested in 1 ml of 16 U/ml papain (P3125, Sigma-Aldrich) in 0.2 M sodium phosphate buffer containing 0.0975 M sodium acetate (W302406, Sigma-Aldrich), 0.0137 M ethylenediaminetetraacetic acid (E6758, Sigma-Aldrich), and 0.005 M cysteine hydrochloric acid (HCl; C1276, Sigma-Aldrich) overnight in a 65°C water bath. The remainder of the assay was conducted per the manufacturer's instructions, and DNA was quantified using the provided standards and normalized to the dry weight of the tissue. A total of n = 3 control NPs and n = 9 decellularized NPs were used for the outlined experiments.

2.1.3 | sGAG content

sGAG content of control and decellularized NP samples was quantified to determine the maintenance of neuroinhibitory components after decellularization. A Blyscan Glycosaminoglycan assay kit (B1000, Biocolor) was utilized according to the manufacturer's instructions. Briefly, lyophilized control and decellularized NP samples were digested in papain as described above (see DNA Content). The remainder of the assay was conducted per the manufacturer's instructions, sGAG was quantified according to the provided standards and normalized to the dry weight of the tissue. A total of n = 3 control NPs and n = 12 decellularized NPs were used for the outlined experiments.

2.1.4 | Collagen content

Maintenance of collagen was determined after decellularization by analyzing collagen content in control and decellularized NP samples. Depending on the type of collagen, hydroxyproline can make up between 12.8% and 14.7% of the mass.[46] A value of 13.5% was used as the percentage of hydroxyproline in collagen. A hydroxyproline assay (ab222941, Abcam) was conducted according to the manufacturer's instructions with slight modifications to determine collagen content. Briefly, lyophilized control and decellularized NP samples

TABLE 1 The time spent in each wash step of the decellularization process

	Wash liquid	Time
1	ddH_20	7 hours
2	100 mM sodium/50 mM phosphate buffer	Overnight (10-12 hours)
3	125 mM SB3-10 in 50 mM sodium/10 mM phosphate buffer	4 hours
4	100 mM sodium/50 mM phosphate buffer	15 minutes
5	3% (w/v) SD/0.6 mM SB-16 in 50 mM sodium/10 mM phosphate buffer	1 hour
6	100 mM sodium/50 mM phosphate buffer	3 × 15 minutes
7	125 mM SB3-10 in 50 mM sodium/10 mM phosphate buffer	1.75 hours
8	100 mM sodium/50 mM phosphate buffer	15 minutes
9	3% (w/v) SD/0.6 mM SB-16 in 50 mM sodium/10 mM phosphate buffer	45 minutes
10	100 mM sodium/50 mM phosphate buffer	3 × 15 minutes
11	DNase (75 U/ml) in 50 mM sodium/10 mM phosphate buffer	34 hours
12	50 mM sodium/10 mM phosphate buffer	3 × 90 minutes
13	1× PBS	3 × 3 hours
14	ddH_2O	3 × 15 minutes
Chemical information for decellularization process		
3-(Decyldimethylammonio)-propanesulfonate inner salt (SB3-10; D4266, Sigma-Aldrich)		
3(N,N-Dimethylpalmitylammonio)-propane inner salt (SB-16; H6883, Sigma-Aldrich)		
Sodium deoxylcholate (SD; D6750, Sigma-Aldrich)		
DNase (D4527, Sigma-Aldrich)		

Abbreviation: PBS, Phosphate-buffered saline.

were digested in 1 ml of 16 U/ml papain (see above) at 65°C overnight. This digested NP was lyophilized overnight to concentrate the tissue. The resulting lyophilizate was hydrolyzed with 200 µl of 5 M sodium hydroxide (NaOH) at 120°C for 1 hour, then neutralized on ice with 200 µl of 5 M HCl. The remainder of the assay was conducted per the manufacturer's instructions, and the resulting data were normalized to the dry weight of the tissue. A total of n = 4 control NPs and n = 4 decellularized NPs were used for the outlined experiments.

2.1.5 | Cytotoxicity of residual chemicals

Cytotoxicity of any residual chemicals in the decellularized NP tissue was evaluated by measuring the change in metabolic activity of human NP cells treated with media eluted from the decellularized NP using the alamarBlue assay (Thermo Fisher, 88 951) in accordance with ISO Standards 10993:5[47] and 10993:12.[48] The alamarBlue assay measures the metabolic activity of cells by reducing resazurin in the electron transport chain to resorufin. This reduction causes a change in color from blue to purple/pink that can be measured. Cells that are more metabolically active will reduce resazurin at a faster rate than less metabolically active cells, leading to a greater color change. Briefly, 100 mg of wet decellularized NP tissue was eluted in 1 ml complete NP media (Sciencell, 4801) for 72 hours at 37°C. Human NP cells (Sciencell, 4800) were grown to passage 4, then split and seeded in a 48-well plate coated with Poly-L-Lysine at a density of 7500 cells/well. The cells were allowed to adhere for 24 hours before they were treated with eluted media. After cells were incubated for 48 hours with the eluted media, alamarBlue reagent was added to each well at a 1:10 ratio and incubated at 37°C for 2 hours. The absorbance of the media was analyzed using a microplate reader (Synergy H1, BioTek, Vermont) at 570 and 600 nm. The reduction of alamarBlue was calculated according to the manufacturer's instructions. All samples including untreated controls were measured in triplicate. A total of n = 3 decellularized spines, with four NP samples taken from each n, for a total of 12 decellularized NP were used in the outlined experiments.

2.1.6 | α-galactose epitope immunostaining

The α-galactosyl epitope (α-gal) content of decellularized NP scaffolds was tested because α-gal is known to elicit an immune response in humans, as humans and old-world monkeys do not express this epitope.[49] Immunostaining was used to test whether the α-gal epitope was present in the NP tissue after decellularization. Fixed control and decellularized NP samples were utilized for α-gal immunostaining. Porcine muscle tissue was used as an additional positive control for α-gal due to its high cellularity and high α-gal presence. After fixation and storage at 4°C in PBS, the PBS was removed, and the tissues were soaked in a 30% sucrose solution at 4°C overnight. The samples were then frozen in optimal cutting temperature compound (4586, Scigen) and cryo-sectioned at 30 µm (CM1950, Leica). Sections were post-fixed to slides in 4% PFA for 30 minutes, followed by 2 × 15-minute washes in 1× PBS and another wash for 15 minutes in PBS with tween (PBST; 0.1% Tween 20 [BP337, Fisher Scientific] in 1× PBS). The sections were then blocked using blocking buffer (3% goat serum; G9023, Sigma-Aldrich), 0.3% Triton X-100 (93443, Sigma-Aldrich) in 1× PBS for 1.5 hours, followed by primary mouse α-gal antibody incubation (ALX-801-090-1, ENZO; 1:1000 in blocking buffer) overnight at 4°C with mild agitation. The sections were washed 6 × 15 minutes in 1× PBST, then incubated with secondary antibody anti-mouse 488 (ab150117, Abcam) for 4 hours at room temperature with mild agitation. The sections were again washed 6 × 15 minutes with 1× PBST. Finally, sections were counterstained with 4′,6-diamidino-2-phenylindole (DAPI) (D1306, Thermo Fisher; 1:1000 in 1× PBS) for 10 minutes, washed 3 × 5 minutes in 1× PBS, mounted using Prolong Gold (P36934, Fisher Scientific) and a glass coverslip. All steps were conducted at room temperature unless otherwise specified. Images were taken using a Zeiss Axio Observer at ×10 magnification and quantified by counting the number of positive α-gal epitopes in three ×10 images of control NP, decellularized NP, and muscle tissue from

three different animals using ImageJ. A total of n = 3 samples were used for each group with a minimum of three images analyzed per n.

2.2 | Creation and characterization of a regelled NP

2.2.1 | Digestion and preparation of decellularized NP gel

The intact AF provides a barrier to delivery to the NP; thus, an injectable formulation is essential. To create an injectable gel made from decellularized NP tissue, previous enzymatic digestion protocols were adapted[50,51]; 20 mg of lyophilized decellularized NP was digested by 1 mg/ml of pepsin (P6887, Sigma-Aldrich) in 0.05 N HCl for 44 hours with spinning at 300 rpm using a magnetic stir bar. Following digestion, all steps of making the regelled NP were performed on ice, until incubation at 37°C. 4-(2-hydroxyethyl)-1-piperazineethanesulfonic acid (HEPES) buffer (H0887, Sigma-Aldrich) was added to attain a concentration of HEPES of 7.5 mM. The digest was then neutralized with 5 M NaOH to pH ~7.4. The digested NP tissue alone did not form a robust gel at 37°C, so type I collagen (354249, Corning) was supplemented to create a more robust gel. Type I collagen was selected because there is an increase in type I collagen with aging, and degeneration forms a gel more consistently than type II collagen. Since the goal of this material is not to regenerate a healthy disc, but rather to act as a neuroinhibitory supplement, collagen type will not impact this property. Dulbecco's Modified Eagle Medium (DMEM; D2429, Sigma-Aldrich) was used to control the ionic strength of the solution, as ionic strength has been demonstrated to have a strong effect on the gelation time, number of fibrils, and size of fibrils of collagen.[52,53] The neutralized tissue digest, as described here after it had been neutralized, was added to premixed tubes containing DMEM and HEPES so that the final concentration of DMEM would be 0.5× and HEPES would be 7.5 mM. Collagen was added last up to a concentration of 2.5 mg/ml. The final pH of the resulting solution was adjusted to ~7.4 using 0.25 M NaOH, and the resulting ionic strength was ~0.148 M. The final formulation with supplemented collagen was termed regelled NP.

2.2.2 | Gelation kinetics

The gelation kinetics, how much the gel absorbs light over time due to fibril formation, and gelation time, at what time the absorbance starts and stops changing, were investigated here; 100 µl of digested NP supplemented with collagen was prepared and pipetted in triplicate into a 96-well plate. The plate was then placed into a microplate reader, preheated to 37°C, and the absorbance was read once every minute for 45 minutes at 405 nm. Gel absorbance was used as an indicator of collagen fibrillogenesis. At this wavelength, the absorbance of the gel depends on the amount of collagen fibril formation.[2] The change in absorbance from the initial value and the normalized absorbance, Equation (1), were calculated to show the percent of the maximum absorbance. A total of n = 3 different preparations were used with three samples analyzed for each n.

$$\mathrm{NA} = \frac{A_2 - A_1}{\mathrm{Max} - A_1}, \tag{1}$$

where NA is the normalized absorbance, A_2 is the absorbance at a specific time, A_1 is the initial absorbance, and Max is the maximum absorbance value over the time course.

2.2.3 | Mechanical characterization

Mechanical characterization including rheology of the gel was performed and compared to previously published data on degenerated NP tissue: a linear compressive modulus of ~5.3 kPa and a complex shear modulus at 1 rad/s of ~17 kPa.[54] Rheology testing was performed on gels using an Anton Paar MCR 302 with sand-blasted plates and a humidity bath. Briefly, regelled NP and collagen control gels were formed by injecting the gel solutions into 8-mm-diameter silicone molds (666305, Grace Bio-Labs), using 21 G needles (305129, BD), between two glass slides and thermally cross-linked at 37°C for 45 minutes. The gels were then allowed to soak in 1× PBS for 30 minutes to become fully hydrated. An initial amplitude sweep was conducted to determine the limiting strain value of the linear viscoelastic region by measuring a shear strain range from 0.001% to 1% with 20 data points, angular frequency of 6.21 Hz, and the reading from 0.1 to 100 rad/s. Following the amplitude sweep, a frequency sweep from 0.1% to 100 rad/s at 0.01% strain, 20 data points were conducted on each gel at 37°C in a humidity bath. Collagen gels with a concentration of 2.5 mg/ml were used as controls. A dynamic shear modulus of $G^* = 17$ kPa and $\tan\delta = 0.3$ at 1 rad/s were used as mildly degenerate human NP rheological values, and $G^* = 7.4$ kPa and $\tan\delta = 0.4$ at 1 rad/s were used as healthy human NP rheological values.[54,55] G^* was calculated as $G^* = \sqrt{G'^2 + G''^2}$ and $\tan\delta = G''/G'$, where G' = storage modulus and G'' = loss modulus. N = 8 collagen control experimental replicates and three regelled NP groups, each with six replicates, for a total of 18 regelled NP samples.

2.2.4 | Scanning electron microscopy

Scanning electron microscopy (SEM) was performed to assess the formation of collagen fibers after NP digestion and regelation. Fixed control NPs, decellularized NPs, and regelled NPs were processed for SEM using a graded dehydration method. Samples were dehydrated in increasing concentrations of ethanol (30%, 50%, 70%, 85%, 90%, 95%, and 100% in ultrapure water) for 15 minutes each at room temperature. Following this, the samples were incubated in increasing percentages of hexamethyldisilazane (HMDS; 16 700, Electron Microscopy Services; 25%, 50%, 75%, and 100% in ethanol) for 30 minutes each at room temperature in a fume hood. Finally, the

samples were submerged in 100% HMDS overnight in a fume hood until the HMDS had completely evaporated. The dehydrated samples were secured to a pin stub mount using conductive tape and sputter coated in platinum/palladium for 20 seconds (106 Autosputter Coater, Cressington). The coated samples were then imaged using an FEI Helios focused ion beam/SEM 660 at a voltage of 5 to 10 kV, current of 0.2 nA, 3 μs dwell time using secondary electron mode, and Everhart-Thornley detector unless through lens detector was needed for finer resolution at higher magnifications. ImageJ was used to quantify the fiber diameter by drawing a line across each distinguishable fiber and measuring the distance of the line. A total of n = 3 different samples were characterized, and at least three images per sample were analyzed for each group at ×100 000 magnification to quantify fiber diameter.

2.3 | NP cell cytocompatibility

2.3.1 | NP cell culture

Human NP cells (4800, ScienCell) were cultured in a T75 flask (CLS430641U, Sigma Aldrich) coated with 15 μg of Poly-L-Lysine (0413, ScienCell). NP cells were cultured in Complete Nucleus Pulposus Cell Media (4801, ScienCell) which was changed every 2 to 3 days. The NP cells were grown to confluency in hypoxia (3.5% oxygen, 10% CO_2, 86.5% N_2) in a modular incubator chamber (MIC-101, Billups-Rothenberg) before being used. Cells from passages 2 and 3 from multiple freeze downs were used in these experiments. These cells were acquired from single, fetal donors, and the identity of the cells was verified by the company through immunofluorescence with antibodies for fibronectin and vimentin (ScienCell).

2.3.2 | 3D cell culture within regelled NP or collagen control gels

NP cells were added to non-cross-linked regelled NP or collagen control solutions to attain a cell concentration of 2 million cells/ml; 30 μl of the gel and cell suspension was transferred to a sheet of parafilm to prevent sticking, then placed in the incubator at 37°C for 40 minutes to cross-link before being transferred individually to 48-well plates; 400 μl of complete NP cell media was added to each well. Media were replaced every 2 to 3 days over the course of 7 days.

An alamarBlue metabolic assay (88951, Thermo Fisher Scientific) was conducted on days 0, 1, 3, and 7 after initiation of culture to determine cell health. At the desired time point, alamarBlue reagent was added to each well at a 1:10 ratio, and the plates were incubated at 37°C in hypoxia for 3 hours; 200 μl of media from each well was moved in duplicate to a 96-well plate. The wells were then rinsed with 1× PBS before adding 400 μl of complete NP media and placing the plates back in the incubator under hypoxia. The absorbance of the removed media was analyzed using a microplate reader at 570 and 600 nm. The reduction of alamarBlue was calculated according to the manufacturer's instructions. The reduction was then normalized to the DNA content of the respective wells, following the conclusion of the experiment. Gels were then frozen in water at −80°C at respective time points for sGAG, collagen, and DNA assays. A total of n = 6 experimental replicates from each preparation, with the collagen having one preparation and the regelled NP having three different preparations for a total of six collagen and 18 regelled NP.

At the study end, all gels were lyophilized overnight. Due to the small masses remaining following lyophilization, the mass could not accurately be determined for normalization. Instead, the data were normalized to each gel, which was a known volume of solution. Three gels from each time point and group were digested in 1 ml of 16 U/ml papain (see above) overnight at 65°C. sGAG, DNA, and hydroxyproline assays were conducted as described previously in Section 2.1. A total of n = 3 experimental replicates from each preparation, with the collagen having one preparation and the regelled NP having three different preparations for a total of three collagen and nine regelled NP.

2.4 | Evaluation of neuroinhibitory properties of regelled NP

2.4.1 | Dorsal root ganglia explant isolation process

Studies using primary rat dorsal root ganglia (DRG) explant culture tested the neuroinhibitory properties of the regelled NP. DRGs are located close to the disc and can sprout pain-sensing neurons into degenerate disc, leading to pain, thus they are an ideal model cell type to validate neuroinhibition in vitro.[4] All animal experiments were conducted in accordance with the Guide for the Care and Use of Laboratory Animals and approved through the University of Nebraska-Lincoln's Institutional Animal Care and Use Committee. Adult male Sprague Dawley rats (CD Rat 001, Charles River) aged 11 to 15 weeks were euthanized, and L1-L6 DRGs were surgically removed and placed in cold trimming media: Neurobasal-A media (10888022, Thermo Fisher Scientific) with 10% fetal bovine serum (FBS; 26140079, Thermo Fisher Scientific), 1% GlutaMax (35050061, Thermo Fisher Scientific), 1% Penicillin/Streptomycin (15140122, Thermo Fisher Scientific), and 2% B-27 Plus Supplement (A3582801, Thermo Fisher Scientific). DRGs were transferred into a 60-mm petri dish with cold trimming media, and excess tissue around the DRG was trimmed using surgical spring scissors under a stereomicroscope (Stemi 508, ZEISS). Trimmed lumbar DRGs were divided into two or three equally sized pieces before culture.

2.4.2 | Gel-within-gel fabrication and DRG explant culture

To accurately model the growth of DRG neurons into a degenerative disc in vitro, we utilized our previously established gel-within-gel 3D culture method to model the in vivo environment of the DRG and

NP.[45] Cut DRGs were embedded and cultured in type I collagen outer hydrogel that surrounded an inner "NP-like" gel. Inner gels consisted of either regelled NP or type I collagen. Collagen inner gels were used as a positive control due to its neuro-permissive properties.[45,56] To prepare the model, regelled NP and collagen gels were prepared as previously described herein with a final collagen concentration of 3.6 mg/ml, to match the final regelled NP collagen concentration which equates to the summation of the added type I collagen (2.5 mg/ml), and the collagen from the digested tissue (1.1 mg/ml).

To form the inner gels, 100 μl of non-cross-linked collagen control or regelled NP was transferred into a 96-well plate with custom laser-cut plastic gel lifters and incubated for 60 to 90 minutes at 37°C, 5% CO_2. The inner gels were carefully lifted out and placed into a 48-well plate using the gel lifters. On ice, 150 μl of the prepared collagen outer gel was then pipetted to the outside of the inner gel, and a DRG explant was carefully embedded in the outer gel, close to the boundary between the two gels. The gel-within-gel was then incubated at 37°C, 5% CO_2, and 95% air for 1 hour to induce collagen gel cross-linking, prior to media addition. The DRGs were cultured in complete media: Neurobasal-A media with 10% FBS, 1% GlutaMax, 1% Penicillin/Streptomycin, 2% B-27 Plus Supplement, and 0.05% NGF (556NG100, Thermo Fisher Scientific) at 37°C and 5% CO_2 for 15 days with half media changes every 3 days. This experiment was repeated three times with at least three inner gels per group. DRGs without any substantial neurite outgrowth in any direction after 15 days in vitro were excluded from this study.

2.4.3 | Neuroinhibition analysis

A total of three experiments with 11 total collagen controls and 20 regelled NP gels were imaged and analyzed. On day 15, DRGs were fixed in 300 μl of 4% PFA for 1 hour at room temperature. DRGs were then washed 3 × 15 minutes with 1× PBS and stored in 1× PBS at 4°C protected from light until immunostaining. Fixed DRGs in gels were stained for neurofilament-H (NF-H). Briefly, the gels were permeabilized in 200 μl of blocking buffer (0.5% Triton X-100, 4% goat serum in 1× PBS) for 1 hour at room temperature. The blocking buffer was removed, and 200 μl of primary antibodies against NF-H (mouse α-NF-H, Ab528399, DSHB; 1:500 in blocking buffer) was added to each well for 36 hours at 4°C. The primary antibody was removed, and the gels were washed 3 × 4 hours in PBST (0.05% Tween 20 in 1× PBS) with mild agitation at room temperature. Secondary antibody (α-mouse 488, ab150117, Abcam; 1:500 in blocking

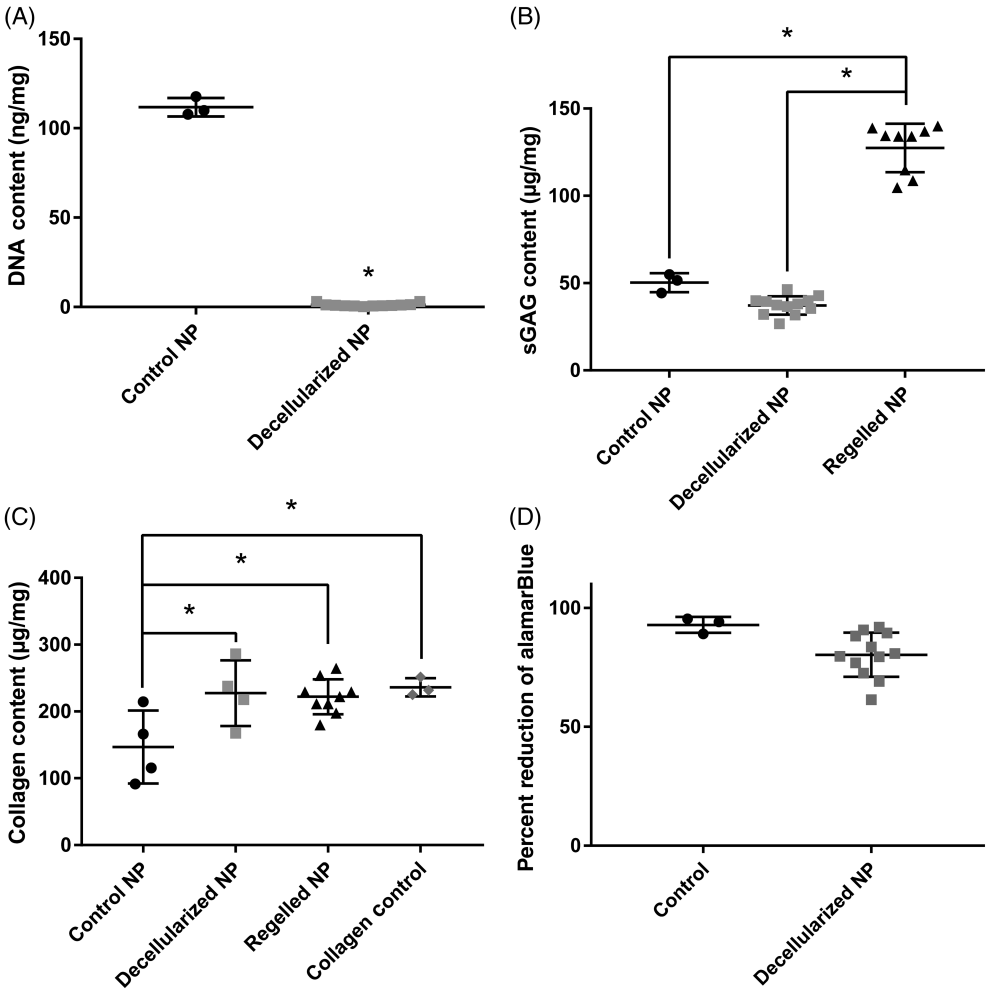

FIGURE 2 The decellularization process removes cells while maintaining extracellular matrix proteins. DNA (A), sGAG (B), and collagen (C) concentrations were compared before and after the decellularization process and after making into a gel. DNA was significantly reduced in the decellularized NP compared to control while sGAG and collagen were maintained. (D) Metabolic activity of NP cells treated with conditioned medium from decellularized NP tissue, normalized to untreated control shows a slight reduction to 86% of the control, which indicates minimal cytotoxic effects. NP, Nucleus pulposus; sGAG, sulfated glycosaminoglycan. *Indicates significant difference $P < .05$

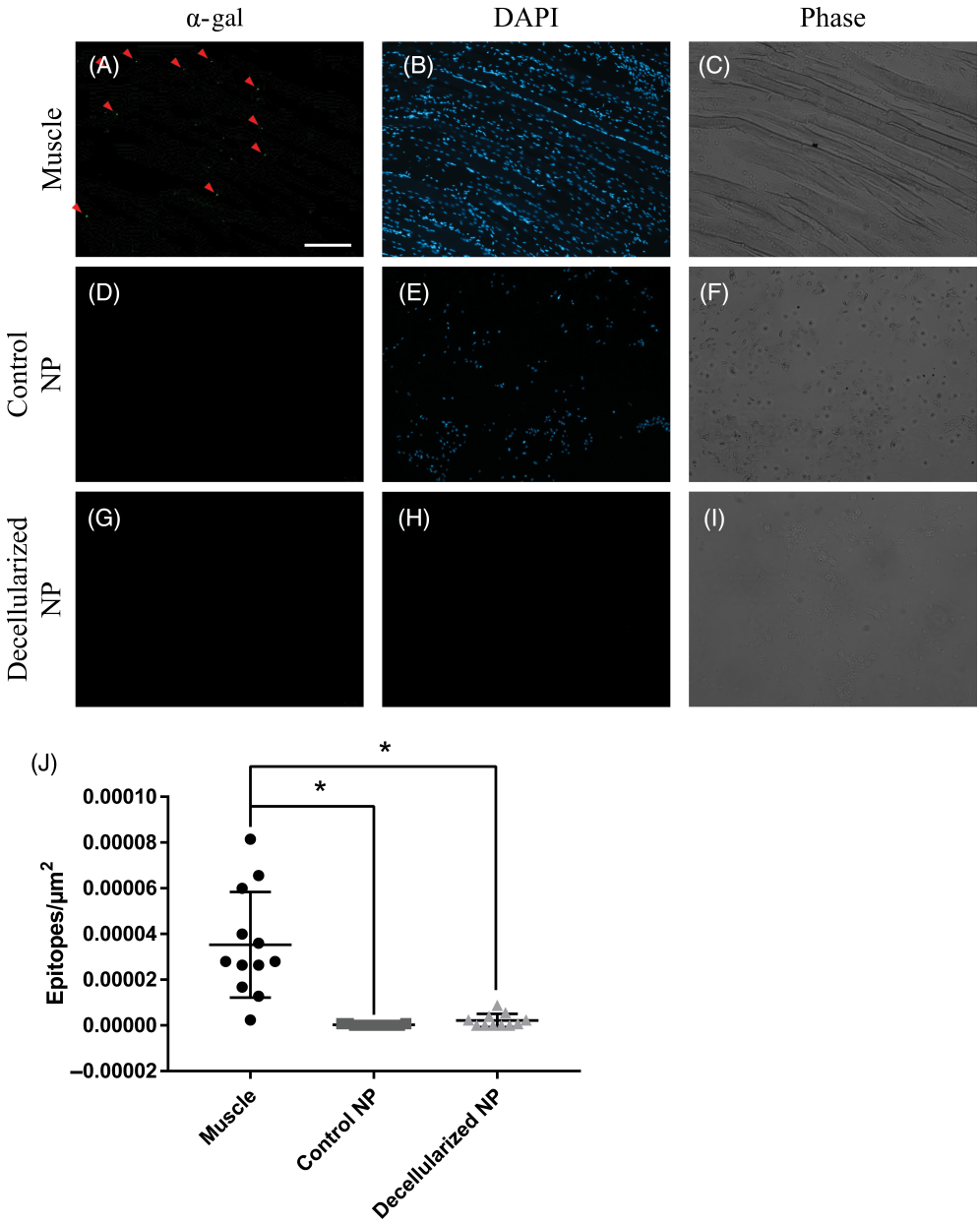

FIGURE 3 Control NP and decellularized NP contain negligible amounts of α-gal antigen. Representative individual channel images for α-gal epitope (green), cell nuclei (blue, DAPI), and phase channels in muscle (A-C), control NP (D-F), and decellularized NP (G-I). Red arrows indicate positive staining for the α-gal epitope. Comparison of number of epitopes normalized to μm^2 in muscle, control NP, and decellularized NP (J). Both the control and decellularized NP had significantly fewer positive α-gal epitopes compared to muscle. Scale bar = 200 μm. NP, Nucleus pulposus. *Indicates significant difference $P < .05$

buffer) was added and incubated overnight at 4°C, protected from light. The secondary antibody was removed, and the gels were washed 3 × 4 hours in PBST at room temperature, with mild agitation, protected from light. The gels were stored in 1× PBS at 4°C, protected from light until imaged. Following staining, the gels were imaged using a widefield fluorescence plate imager (Cytation 1, BioTek) at 488 nm to visualize the neurons. Representative images were taken on a ZEISS Confocal microscope LSM 800. Brightfield photos of the gel-within-gels were taken using a digital camera (EOS Rebel T6i, Canon) attached to a stereomicroscope (Stemi 508, Zeiss).

Using Adobe Photoshop CC 2019, the brightfield images were overlayed over the fluorescent images taken from the Cytation plate imager and gel boundaries were drawn. Gels without distinct boundaries were excluded from the analysis. ImageJ software, Simple Neurite Tracer tool, and a modified Sholl analysis were used to quantify the: (1) maximum radial distance, (2) total distance traveled in the inner gel, (3) number of neurites extending within the inner gel at specific distances from the gel boundary, and (4) the number of neurites extending away from the inner gel at specific distances from the DRG body.[45] The maximum radial distance was determined by drawing a straight line from the tip of the longest neurite to where it initially crosses the gel boundary. The maximum neurite length was determined by tracing the longest nerves using the simple neurite tracer tool up until the gel boundary. Only the largest values were used from each image for both the radial distance and neurite length. Sholl analysis has previously been used to determine the amount of neurite branching based on distance from the cell body.[57,58] This method was modified here to represent the distance from the boundary of the inner and outer gels as well as the number of neurites growing away from the DRG body. Sholl analysis was able to determine the number of neurites at a given distance from the gel boundary. A total of n = 3 experiments were conducted with at least three replicates per condition in each experiment.

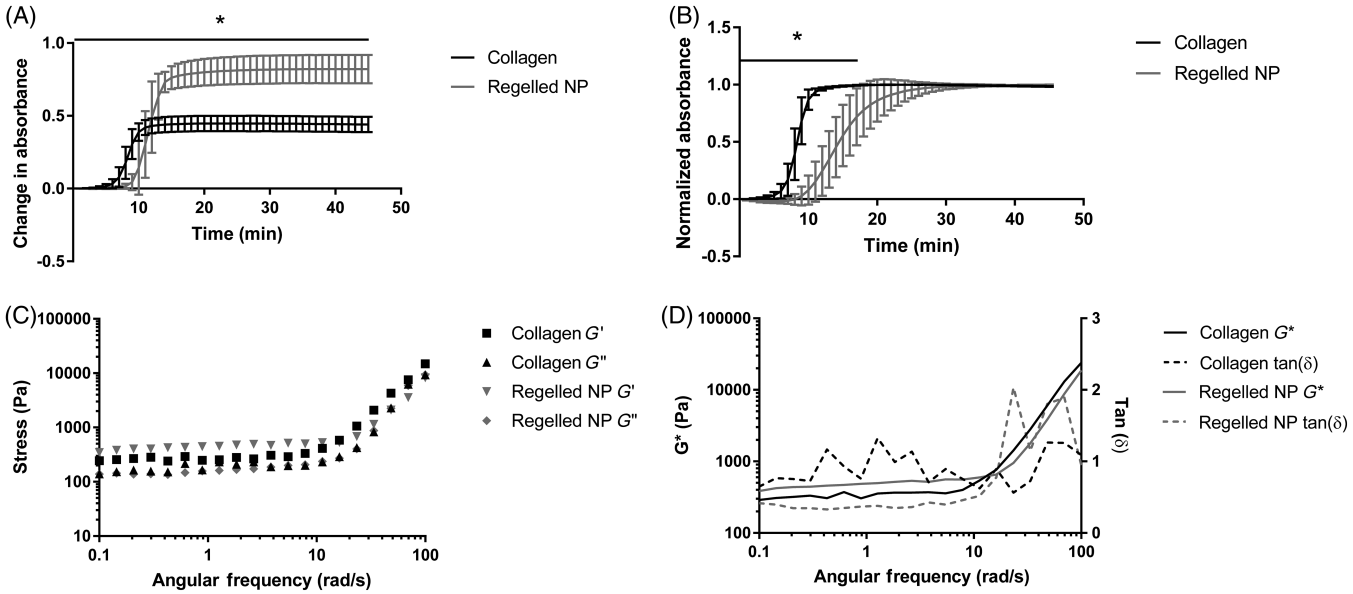

FIGURE 4 Gelation and mechanical properties of the regelled NP compared to collagen controls. A, The change in absorbance measured over time of collagen and regelled NP demonstrate a large and significant difference, suggesting that the regelled NP becomes more opaque than collagen. B, The normalized absorbance of the gels suggests that collagen only reaches its maximum value much sooner than the regelled NP. C, Rheology comparing the storage (G′) and loss (G′′) moduli between collagen and regelled NP suggests that regelled NP is weaker than collagen. There were no significant differences between the G′′ of either group, but the G′ of collagen was significantly different than that of regelled NP at 69.5 and 100 rad/s. D, Rheology comparing the dynamic shear modulus (G*) and tan δ of collagen and regelled NP suggests that regelled NP is weaker than collagen. G* of collagen was significantly different from that of regelled NP at 69.5 and 100 rad/s while tan δ was significantly different at 23.4 rad/s. Error bars were omitted from C and D to improve clarity. NP, Nucleus pulposus

2.5 | Statistical analyses

Statistical analysis was conducted using the GraphPad Prism 7.03 software. Statistical significance was determined in the DNA experiment on the decellularized tissue between the control and the treatments using an unpaired Welch's unequal variances *t* test. Statistical significance was determined in the sGAG, collagen, α-gal, and SEM fiber diameter experiments using a one-way analysis of variance (ANOVA) with multiple comparisons with Tukey's post hoc test. A two-way ANOVA with multiple comparisons between days (Sidak's post hoc test) and within each treatment group (Tukey's post hoc test) was used to determine significance for the DNA, sGAG, collagen, and alamarBlue assays in the NP cell culture in gels. In the neuroinhibition experiments, Welch's unequal variances *t* tests were used for the maximum neurite length, maximum radial distance analyses, and distance of the DRG from the boundary, while a two-way ANOVA with multiple comparisons and Sidak's post hoc test was used for the Sholl analysis to determine significance. Significance was set as $P \leq .05$ for all analyses. Error bars for all graphs represent the SD.

3 | RESULTS

3.1 | Validation of whole disc decellularization methods

The PicoGreen assay demonstrated 99.0% reduction in DNA in the decellularized NP samples compared to the control NP tissue, with the decellularized NP samples having a normalized DNA content of 1.19 ± 0.94 ng DNA/mg tissue compared to 111.78 ± 5.18 ng/mg in the control NP, suggesting that native cells and antigens were successfully removed (Figure 2A). The Blyscan assay demonstrated retention of 74.0% of sGAGs in the decellularized NP compared to the control NP samples, with control NP samples having sGAG content of 50.27 ± 5.40 μg/mg and the decellularized NP samples having 37.19 ± 5.27 μg/mg (Figure 2B). The hydroxyproline assay results suggested that collagen took up a greater proportion of the total mass of the decellularized NP compared to control NP (146.9 ± 54.7 control NP vs 227.3 ± 49.1 μg/mg decellularized NP); however, the decellularized and control NP were not significantly different from each other (Figure 2C). Enrichment of collagen in decellularized NP compared to control NP was due to removal of cells and other antigens thereby reducing the overall mass while maintaining the amount of collagen in the tissue. The ratio of sGAG:hydroxyproline was calculated to be 10.16:1 in control tissue and 4.85:1 in decellularized NP.

Cytotoxicity of remaining chemicals after decellularization was tested using an alamarBlue assay to measure the metabolic activity of NP cells treated with eluted media from decellularized NP samples compared to control NP cells with normal growth media. Control NP cells exhibited a reduction of alamarBlue of 92.8 ± 3.36%, whereas NP cells treated with eluted media had a reduction of alamarBlue of 80.28 ± 9.30%, which is a significant difference. When normalized to control, NP cells treated with eluted media had a metabolic activity of 86.5 ± 10.0% (Figure 2D). The eluted NP cells have a 14% reduction in metabolic activity, which is below the recommended value by ISO

10993:5 for cytotoxicity.[47] Cytotoxicity of the final regelled NP on DRG cultures was assessed below during neuroinhibition studies.

α-gal epitopes are an antigen that is present in porcine tissue, but not humans, so lack of removal can cause an immune response. Quantification of α-gal epitopes revealed very few α-gal epitopes were present in either the control or decellularized NP samples. Figure 3A-I shows representative images of α-gal in muscle, control NP, and decellularized NP. Analysis of α-gal epitopes (Figure 3J) revealed there was a significant reduction in the number of α-gal epitopes in the control NP samples and decellularized NP samples compared to the muscle tissue but no difference between control and decellularized NP.

3.2 | Creation and characterization of regelled NP

The normalized gel absorbance was used to determine the start and end of the gelation process. Collagen gels started and finished forming before the regelled NP, starting at 3 minutes, and reaching 95% of its maximum value after 12 minutes. The regelled NP started forming later at 8 minutes and reached 95% of its maximum value after 17 minutes (Figure 4A,B). Results from rheological analysis of the regelled NP and control collagen displayed a stable dynamic shear modulus (400-530 Pa and 300-400 Pa, respectively) and tan δ (0.4-0.7 for both regelled NP and collagen) from 0.1 to 20 rad/s followed by an increase up to 100 rad/s, where all samples had a dynamic shear modulus of ~11 000 to 12 000 Pa and a tan δ of 0.72 to 1.4 for the regelled NP and 17 500 Pa and a tan δ of 0.63 for the collagen (Figure 4D). In comparison, human NP ranges in dynamic shear modulus from 7.4 to 19.8 kPa and tan δ of 0.424 to 0.577.[54,55,59]

SEM imaging revealed that collagen gels tended to have smaller, less organized fibers, compared to the other gels whereas control NP tissue had thicker, more dense collagen fibers, as well as cell debris covering much of the fiber surface (Figure 5A-H). Decellularized NP had a looser fiber network, and the fibers were not as entangled compared to the other gels. The final regelled NP had thick fibers, similar to control NP, although fibers were less dense, more similar to decellularized NP. The diameters of the fibers were quantified for each group and were found to have no significant differences between any group, although regelled NP tended to have slightly thicker fibers compared to the other groups (Figure 5I).

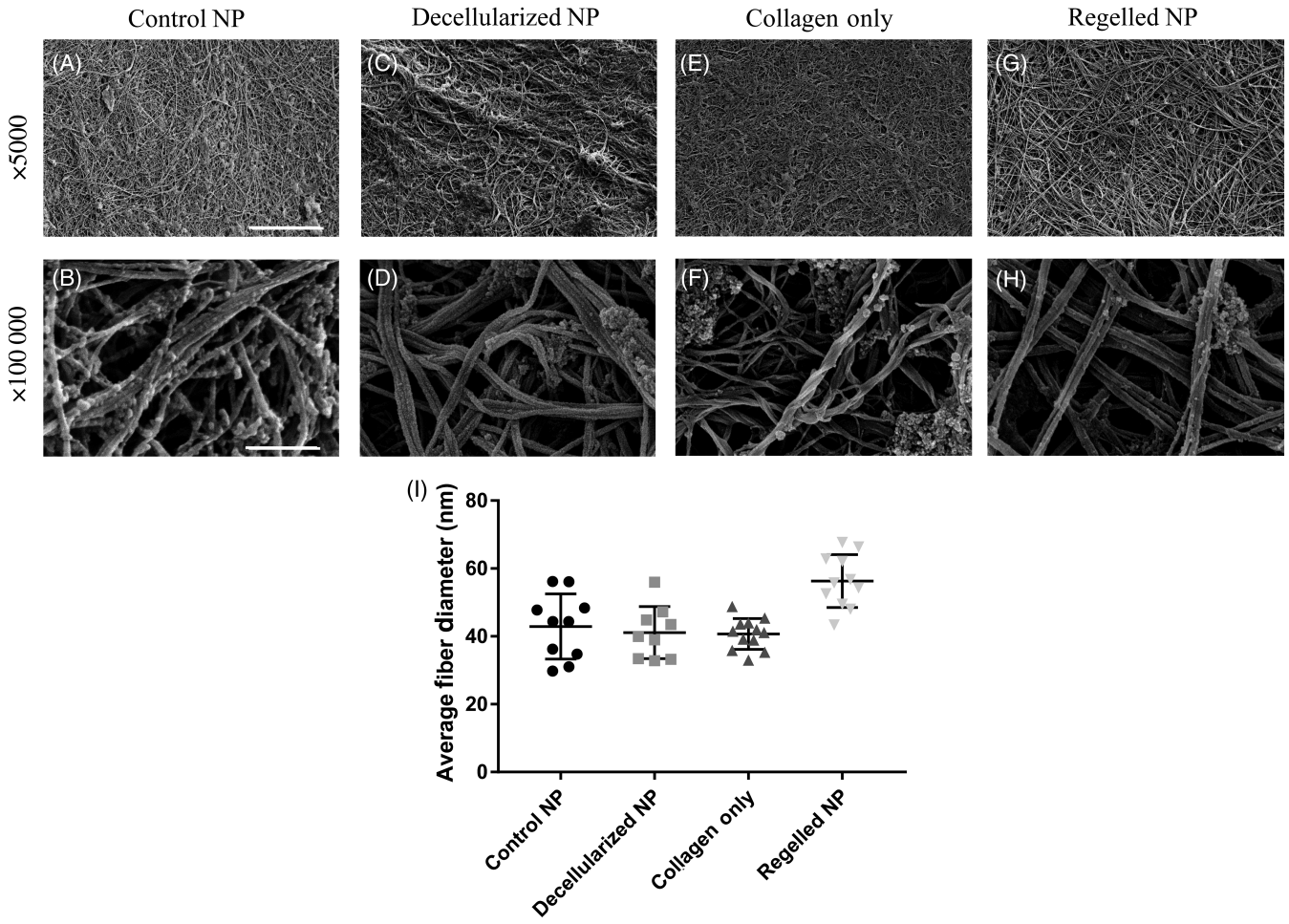

FIGURE 5 Scanning electron microscope images show similar fiber thickness between control NP (A, B), decellularized NP (C, D), collagen only (E, F), and regelled NP (G, H). Quantification of fiber diameter between groups. There were no significant differences between any group (I). Scale bar = 10 μm for ×5000 and 0.5 μm for ×100 000. NP, Nucleus pulposus

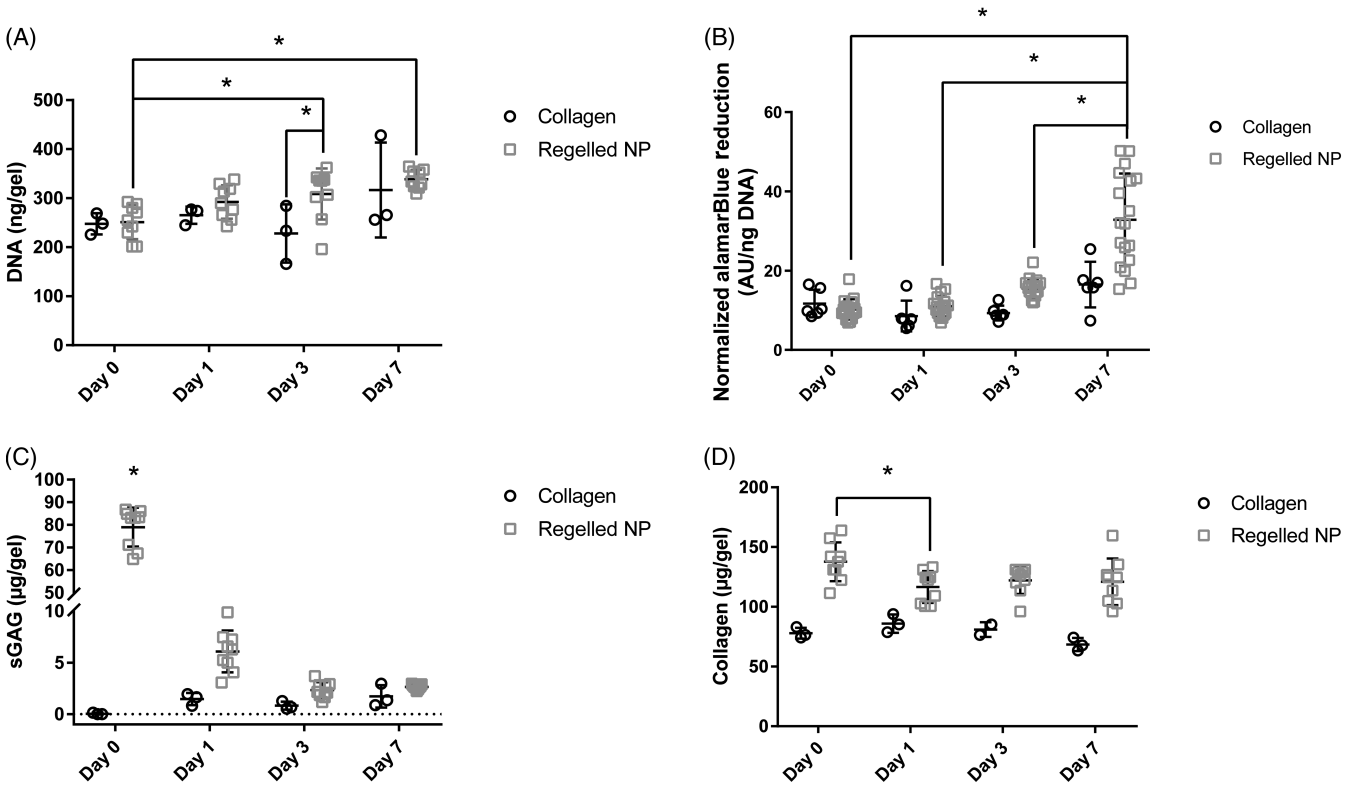

FIGURE 6 NP cells remain viable in regelled NP gels over 7 days and become more active compared to collagen. PicoGreen DNA results (A) demonstrated an increase from day 0 to 7 in the regelled NP groups, while collagen on day 3 was decreased. AlamarBlue (B) showed a significant increase in metabolic activity of each group of gels normalized to DNA on day 7 in the regelled NP gels to all other time points. The regelled NP groups were also significantly greater than the collagen group on day 7. The sGAG quantification (C) revealed a significant decrease in the regelled NP groups from day 0 to the following days; however, all groups appeared to increase in sGAG from day 3 to 7, although not significant. Quantification of collagen content (D) was stable over time in both groups, with only days 0 and 1 in the regelled NP group being significantly different. The collagen control group was significantly lower than the regelled NP at each time point. NP, Nucleus pulposus; sGAG, sulfated glycosaminoglycan. *Indicates significant difference $P < .05$

Regelled NP exhibited significant increases in DNA on days 3 and 7 compared to day 0, while the collagen group was significantly lower than the regelled NP group on day 3 (Figure 6A). Increasing DNA indicated the gels do not inhibit cell proliferation. Normalized alamarBlue results showed that metabolic activity of human NP cells on day 7 cultured in regelled NP was significantly higher than every other day of that same gel (Figure 6B). Normalized metabolic activity for day 7 regelled NP was also significantly greater than the day 7 collagen (Figure 6B). The results of sGAG quantification reveal that regelled NP samples have a large amount of sGAG at day 0, which reduced over the first 3 days and subsequently starts to slowly increase over time, although not significantly (Figure 6C). The control collagen gels have low sGAG that gradually increased over time, although not significantly. The hydroxyproline assay demonstrated a significant but minor decrease between days 0 and 1 in the regelled NP group, but there were no other differences within either group over the time course (Figure 6D). The collagen group was significantly lower than the regelled NP group at each time point but also did not exhibit any differences over the time course. These data demonstrate a constant collagen content over the 7-day time course for both samples. The sGAG:hydroxyproline ratio on day 0 was 4.25:1 and reduced to 0.162:1 by day 7.

3.3 | Evaluation of neuroinhibitory properties of regelled NP

DRG neuroinhibition results demonstrated a significant reduction in the number and distance of neurites growing into regelled NP compared to collagen controls. Figure 7 shows representative images of DRGs cultured in the gel-within-gel model on day 15, with fluorescent staining of the neurites with NF-H. Figure 8A,B shows representative images of the neurite length analysis. Maximum neurite length in the inner gels was lower in regelled NP compared to collagen controls (1201.1 ± 258.3 vs 1763.9 ± 407.5 µm) although this difference was not significant (Figure 8C). Figure 8D,E shows representative images of the radial distance. Analysis revealed there was a significant reduction in the maximum radial distance, or the linear distance from the neurite crossing the boundary to the tip, of neurites in regelled NP samples compared to collagen controls (975.9 ± 41.64 vs 1601.3 ± 381.1 µm) (Figure 8F). Figure 8G, H shows representative images of the Sholl analysis, which found that there were significantly fewer neurons in the regelled NP compared to collagen at all distances up to 700 µm away from the gel boundary, except at 600 µm (Figure 8I). The second Sholl analysis demonstrated no significant differences in the number of neurites between collagen

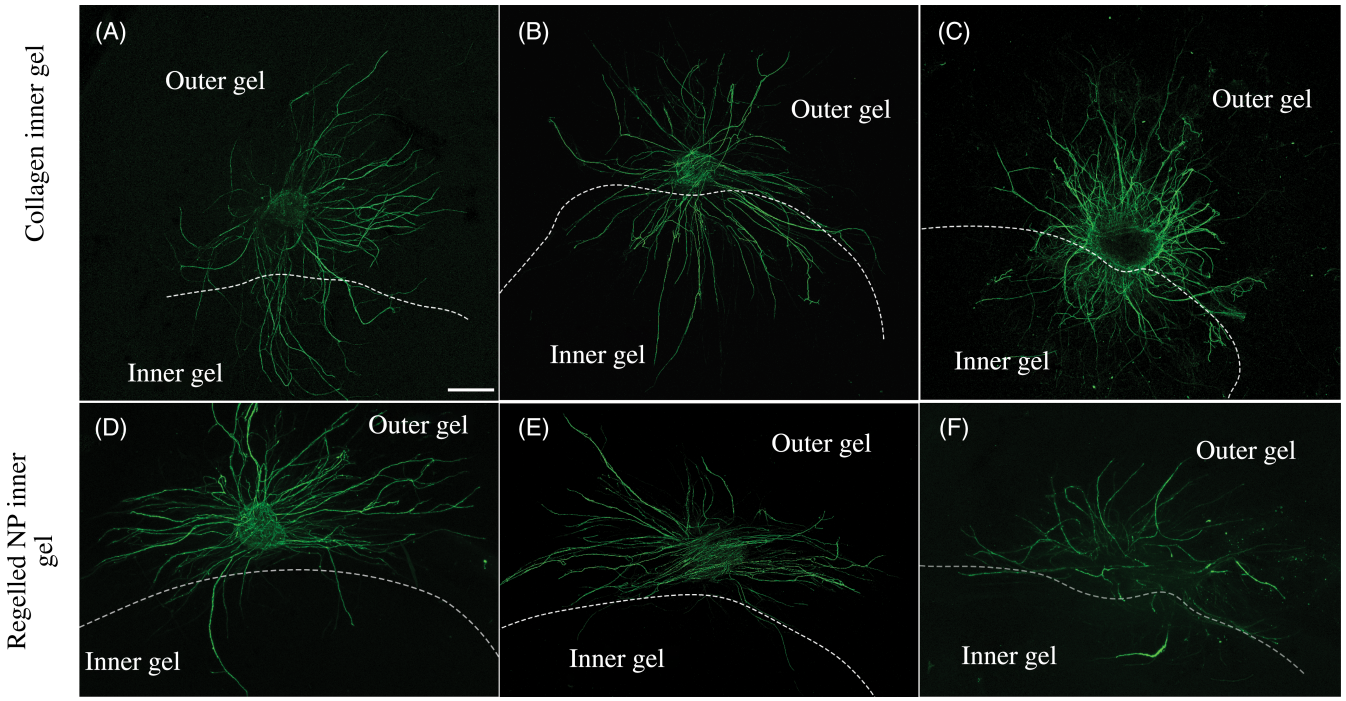

FIGURE 7 DRGs show reduced growth and altered morphology into the inner gel in regelled NP compared to collagen. Representative maximum projection confocal images of day 15 DRGs in regelled NP gels (D-F) and collagen gels (A-C). Scale bar = 500 μm. DRG, Dorsal root ganglia; NP, nucleus pulposus

or regelled NP at any distance on the opposite side of the inner gel. The average distance of the DRGs from the boundary of each group was also calculated as 278.4 ± 118.3 μm for collagen and 244 ± 140.9 μm for regelled NP. These distances were not significantly different from each other. These data indicate that any residuals left in the regelled NP are not cytotoxic to neurons and their support cells in culture. Taken together, these data demonstrate the regelled NP has robust neuroinhibitory properties compared to collagen controls.

4 | DISCUSSION

Previous publications have developed NP decellularization methods with varying success in the removal of DNA and maintenance of extracellular matrix proteins.[38-44] Some of these decellularization techniques have demonstrated high maintenance of glycosaminoglycans, key components of the NP that help to maintain osmotic pressure as well as provide the NP with neuroinhibitory properties, yet no literature has demonstrated maintenance of the neuroinhibitory properties of the decellularized scaffold. In this study, we successfully optimized a high-throughput decellularization process for whole porcine NP, created a thermally gelling hydrogel from the decellularized NP, and demonstrated the regelled NP gels maintain cell viability and prevent nerve growth to be used as a neuroinhibitory supplement for the NP.

To date, no one has explored neuroinhibitory properties of decellularized NP tissue. To investigate the neuroinhibitory properties of our regelled NP, we used our in vitro model of innervation that involves culturing whole DRGs in an outer gel and allows the nerves to grow into an inner gel. In this study, the inner gel was composed of either the regelled NP or a matched collagen control gel. These data demonstrated that the regelled NP was significantly more neuroinhibitory than collagen control gels. We used three different methods to analyze nerve growth into the inner gels and determined significant differences in the maximum radial distance and total number of nerves sprouting within the inner gels at varying depths. Maximum neurite length analysis demonstrated a decrease in the neurite length in the inner gel of regelled NPs; however, this was not significant compared to collagen controls. The results of the neuroinhibition experiments demonstrate that regelled NP exhibits robust neuroinhibitory properties. There are several factors that contribute to neuroinhibition in the body. The first contributing factor to neuroinhibition is the stiffness of the material that the nerve is growing into.[60] Our rheology data indicate that regelled NP and collagen have similar mechanical properties; therefore, mechanics is likely not a major contributor to the neuroinhibition seen in the regelled NP compared to collagen. The next contributing factor to neuroinhibition is the porosity of the material.[61] A porosity of ~80% was shown to promote the greatest nerve density and length with these values decreasing at 70% and 90% in a rat hemisection lesion.[61] SEM analysis revealed no significant difference in fiber diameter. Although porosity cannot be calculated from SEM images, macroscopic evaluation of fibers and void space suggests similar fiber density and thus likely similar porosity between all groups. Another factor contributing to neuroinhibition is the presence of neuroinhibitory molecules in

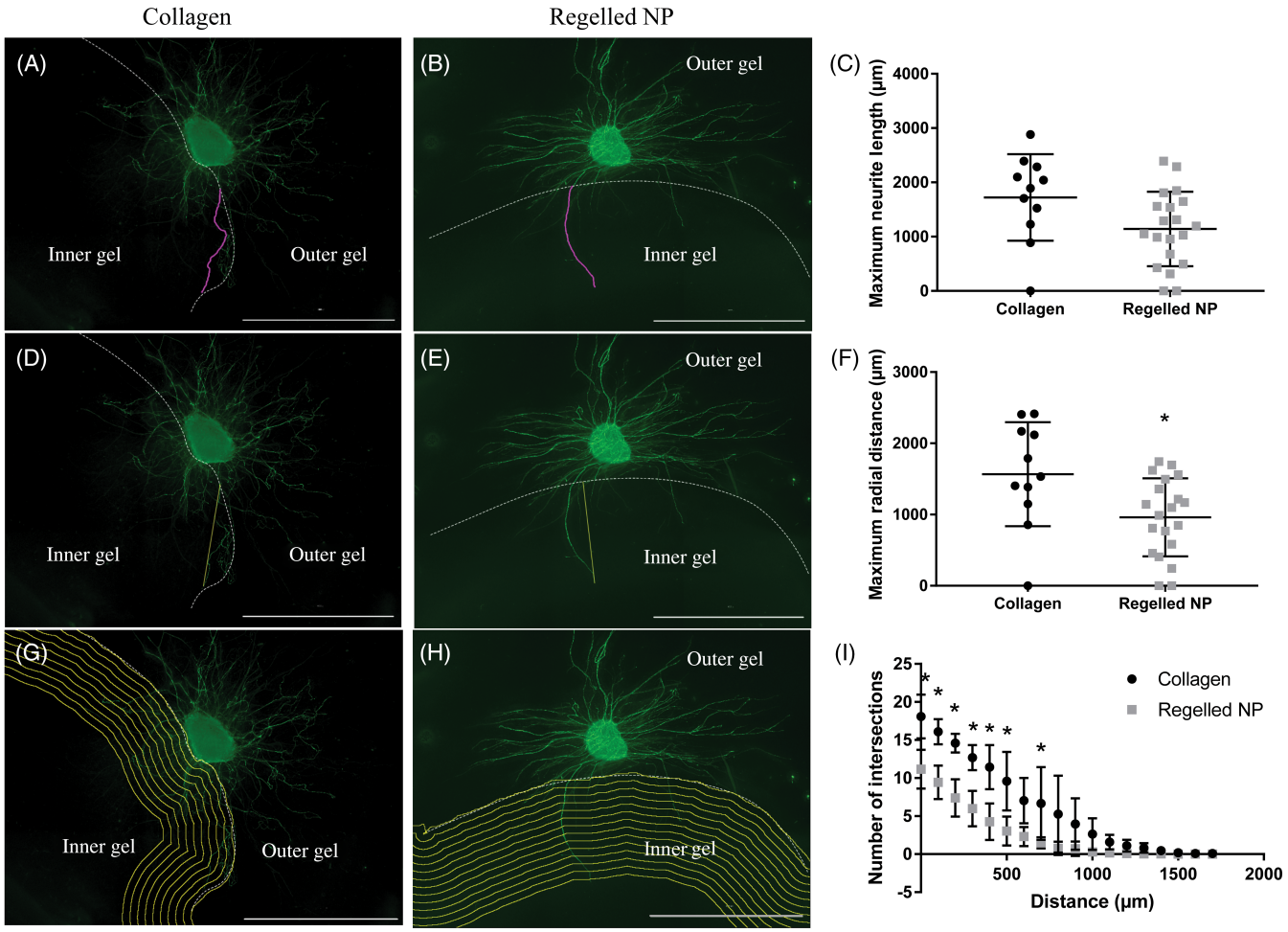

FIGURE 8 Neurite growth into regelled NP inner gels is significantly inhibited compared to collagen inner gels. Representative images (A,B) and analysis (C) for maximum neurite length into the inner gels. Representative images (D, E) and analysis (F) for maximum radial distance into the inner gels. Representative images of Sholl analysis (G,H) and quantification of the number of neurons at specific distances into the inner gel (I). Graphs C and F show the average and SD of the gels individually to show the scattering of the individual points. Scale bar = 2000 μm. NP, Nucleus pulposus. *Indicates significant difference $P < .05$

the material. Some common neuroinhibitory molecules include aggrecan, a proteoglycan present in the NP, chondroitin-6-sulfate, a major sGAG found on proteoglycans in the NP, and semaphorin3A, an axon guidance molecule in the nervous system.[23,24,62] While aggrecan and chondroitin-6-sulfate have been found in large quantities in the NP, semaphorin3A is demonstrated more in the outer AF with ~80% of cells expressing it, with a decreasing concentration into the NP, and with only ~5% of cells expressing it.[62] Given that our regelled NP likely includes higher amounts of these neuroinhibitory molecules than type I collagen, we believe that the presence of sGAGs and semaphorin 3A likely contributes to the neuroinhibitory properties of the regelled NP. However, additional studies are needed to validate this claim.

Several studies have found that most painful, degenerate discs contain nerves, due to a loss in neuroinhibition.[25-27] Reintroducing a neuroinhibitory gel has the potential to stop further ingrowth of nerves and halt the progress of disc-associated LBP. The removal of cellular DNA is crucial to the decellularization process to prevent an immune response when applied in vivo. It is speculated that during degeneration, there is infiltration of immune cells, which can recognize foreign cellular components and cause a host to reject the implanted material.[63] Thus, our removal of more than 99% of the original DNA from the tissue, as an indicator for cells, increases the chances of a host accepting the decellularized tissue in the future. Due to the high removal of DNA and lack of α-gal found within the decellularized NP, it is unlikely that this tissue would cause an immune response due to species differences when implanted in a host. Porcine tissue has had clinical success previously with dermis (Fortiva) and small intestinal submucosa (Cook Biotech), suggesting that porcine NP may also be implanted without problem after decellularization. Besides DNA removal, the other important aspect of decellularization is the maintenance of native proteins. In the NP, the majority of the extracellular matrix is composed of sGAGs and type II collagen.[64,65] The decellularization process used here attempted to maintain as much of the native sGAGs and collagen as possible, to maintain the neuroinhibitory and structural capabilities of the tissue. Here, the sGAG maintenance was 74.0%, comparable to other NP decellularization processes that have a range of retentions between

55% and 97%.[2,38-44] To compare the normalized sGAG values to previous literature, the values of 50.27 ± 5.40 μg/mg and 37.19 ± 5.27 μg/mg for control and decellularized NP, respectively, are generally lower than other work, which range from ~20 μg/mg to ~575 μg/mg.[2,38-44] The large difference in sGAG content may be due to differences in species, age of the NP donor, and disc level of the decellularized NP. Healthy human NP tissue tends to have an sGAG concentration of 440 μg/mg, while degenerate tends to have approximately 150 μg/mg.[66] The regelled NP had similar levels of sGAG to that of degenerate NP; however, it appears that the regelled NP exhibited neuroinhibitory properties while degenerate NP does not. A common comparison used in NP decellularization is the ratio of sGAG:hydroxyproline. Here, this ratio was 10.16:1 in control tissue, 4.85:1 in decellularized NP, and 4.25:1 in the regelled NP. These results suggest that the regelled NP is similar to the ratio of sGAG to collagen to decellularized NP tissue. Because the regelled NP is meant as a neuroinhibitory supplement, the sGAG:hydroxyproline ratio does not need to reach back to natural tissue. Further, our SEM images illustrated collagen fibers of similar orientation and thickness at each stage of the decellularization process, suggesting that our process retains the microstructure of a native NP.

Following decellularization, we were able to form digested NPs using an enzyme digestion process followed by collagen supplementation, which can then be injected through a small-bore needle and gel at 37°C in 10 to 20 minutes to create the regelled NP. The metabolic activity of the cells in the regelled NP increased over time compared to the collagen group, with a significant difference by day 7, suggesting that the cells in the regelled NP are more active compared to the collagen group. This may be due to the cells recognizing the decellularized tissue and acting on cues that the tissue gives the cells, whereas the collagen gel would not have these same cues due to the lack of decellularized tissue. Similar phenomena have been demonstrated with cells on other decellularized tissues, with increases in metabolism by these cells when cultured on the decellularized tissue.[67,68] Increases in anabolic gene expression have also been demonstrated with stem cells cultured on decellularized NP tissue compared to controls, which would suggest an increase in metabolism as well.[42,44] The DNA assay showed a small but significant increase over time in the concentration of DNA in the regelled NP compared to collagen controls that suggests that there was minimal cell death, and the cells continued to proliferate over the course of the study. The significant increase in DNA in the regelled NP but not the collagen over 7 days suggests that some components in the decellularized NP is giving cues to the NP cells to proliferate, as the presence of decellularized tissue was the only difference between the two groups. Interestingly, there was a significant decrease in sGAG observed from day 0 to 1. This may be due to the diffusion of the sGAGs into the media due to the large surface area exposed to media in the 30 μl gels. Our regelled NPs cultured with sensory neuron studies still exhibited robust neuroinhibitory properties, suggesting the resultant sGAG loss is either less in these larger gels, or the loss is not sufficient to reduce neuroinhibitory properties. It is not anticipated that diffusion will have a large impact in vivo, due to the enclosed environment of the NP. However, it is possible that sGAG will continue to diffuse out from the gel, which may inhibit the efficacy of the regelled NP in the long term. Future work will examine the function of these scaffolds in vivo to verify efficacy. In conjunction with the sGAGs, the levels of collagen were also investigated over time and showed few differences, with only days 0 and 1 in the regelled NP being significantly different. Between groups, the collagen and the regelled NP were significantly different at each time point, due to the collagen found naturally in the decellularized NP. Taken together, these results indicate that the regelled NP is not cytotoxic and may promote enhanced cell proliferation and remodeling compared to collagen gels.

While the regelled NP has promise for preventing nerve growth in the disc, there are also some limitations. These include the regelled NP's low mechanical properties compared to human NP, which ranges in dynamic shear modulus from 7.4 to 19.8 kPa and tan δ of 0.424 to 0.577,[54,55,59] suggesting this material must be used in conjunction with native tissue to bear load. While these data suggest that the mechanical properties of the regelled NP are lower than native tissue, this is not a large limitation because this gel is meant to act as a supplement to the NP, and not a total replacement. Another limitation of this research was the loss of sGAG from day 0 to 1 in the regelled NP during the 3D culture, which was most likely due to washing out of unbound sGAG during media changes due to diffusion; however, this did not seem to impact the neuroinhibition results. Another limitation of this work was that the regelled NP did not exhibit complete neuroinhibition, only partial, as some of the DRG neurites were still able to pass the inner gel boundary. This feature will be investigated in the future by determining if neurites are traveling along the top or bottom of the gels instead of traveling through the gel. Supplementation of sGAG to the regelled NP may be possible to boost the regelled NP's neuroinhibitory properties. Future work will investigate the effects of this gel on cultured stem cells and the gel's ability to differentiate stem cells toward an NP-like phenotype for NP regeneration as well as the effects of LBP alleviation in vivo.

ACKNOWLEDGMENTS

The research was funded in part by the Nebraska Tobacco Settlement Biomedical Research Development Fund. The research was performed in part in the Nebraska Nanoscale Facility: National Nanotechnology Coordinated Infrastructure and the Nebraska Center for Materials and Nanoscience (and/or NERCF), which are supported by the National Science Foundation under Award ECCS: 1542182, and the Nebraska Research Initiative. The authors acknowledge the US Meat Animal Research Center abattoir staff for assistance in collecting the porcine spinal tissue.

CONFLICT OF INTEREST

The authors declare there are no conflicts of interest.

ORCID

Logan M. Piening https://orcid.org/0000-0003-2428-7934
Rebecca A. Wachs https://orcid.org/0000-0001-5735-6284

REFERENCES

1. National Institute of Neurological Disorders and Stroke, Low back pain fact sheet, 2020. https://www.ninds.nih.gov/Disorders/Patient-Caregiver-Education/Fact-Sheets/Low-Back-Pain-Fact-Sheet.
2. Wachs RA, Hoogenboezem EN, Huda HI, Xin S, Porvasnik SL, Schmidt CE. Creation of an injectable in situ gelling native extracellular matrix for nucleus pulposus tissue engineering. *Spine J*. 2017;*17*(3):435-444.
3. Navani A, Manchikanti L, Albers SL, et al. Responsible, safe, and effective use of biologics in the management of low back pain: American Society of Interventional Pain Physicians (ASIPP) guidelines. *Pain Physician*. 2019;*22*(1):S1-S74.
4. Binch AL, Cole AA, Breakwell LM, et al. Nerves are more abundant than blood vessels in the degenerate human intervertebral disc. *Arthritis Res Ther*. 2015;*17*(1):1-10.
5. Wu B, Yang L, Peng B. Ingrowth of nociceptive receptors into diseased cervical intervertebral disc is associated with discogenic neck pain. *Pain Med*. 2019;*20*(6):1072-1077.
6. Park E, Moon S, Suh H, et al. Disc degeneration induces a mechanosensitization of disc afferent nerve fibers that associates with low back pain. *Osteoarthr Cartil*. 2019;*27*(11):1608-1617.
7. Freemont A, Watkins A, Le Maitre C, et al. Nerve growth factor expression and innervation of the painful intervertebral disc. *J Pathol*. 2002;*197*(3):286-292.
8. Kalakoti P, Missios S, Maiti T, et al. Inpatient outcomes and postoperative complications after primary versus revision lumbar spinal fusion surgeries for degenerative lumbar disc disease: a national (nationwide) inpatient sample analysis, 2002–2011. *World Neurosurg*. 2016;*85*:114-124.
9. Ibrahim T, Tleyjeh I, Gabbar O. Surgical versus non-surgical treatment of chronic low back pain: a meta-analysis of randomised trials. *Int Orthop*. 2008;*32*(1):107-113.
10. Beckerman D, Esparza M, Lee SI, et al. Cost analysis of single-level lumbar fusions. *Global Spine J*. 2020;*10*(1):39-46.
11. Engsberg JR, Lenke LG, Reitenbach AK, Hollander KW, Bridwell KH, Blanke K. Prospective evaluation of trunk range of motion in adolescents with idiopathic scoliosis undergoing spinal fusion surgery. *Spine*. 2002;*27*(12):1346-1354.
12. Katsuura A, Hukuda S, Saruhashi Y, Mori K. Kyphotic malalignment after anterior cervical fusion is one of the factors promoting the degenerative process in adjacent intervertebral levels. *Eur Spine J*. 2001;*10*(4):320-324.
13. Goffin J, Geusens E, Vantomme N, et al. Long-term follow-up after interbody fusion of the cervical spine. *J Spinal Disord Tech*. 2004;*17*(2):79-85.
14. Raj PP. Intervertebral disc: anatomy-physiology-pathophysiology-treatment. *Pain Pract*. 2008;*8*(1):18-44.
15. Adams MA, Roughley PJ. What is intervertebral disc degeneration, and what causes it? *Spine*. 2006;*31*(18):2151-2161.
16. Grunhagen T, Wilde G, Soukane DM, Shirazi-Adl SA, Urban JP. Nutrient supply and intervertebral disc metabolism. *JBJS*. 2006;*88*(suppl_2):30-35.
17. Maroudas A, Stockwell R, Nachemson A, Urban J. Factors involved in the nutrition of the human lumbar intervertebral disc: cellularity and diffusion of glucose in vitro. *J Anat*. 1975;*120*(Pt 1):113-130.
18. Nachemson A, Lewin T, Maroudas A, Freeman M. In vitro diffusion of dye through the end-plates and the annulus fibrosus of human lumbar inter-vertebral discs. *Acta Orthop Scand*. 1970;*41*(6):589-607.
19. Benneker LM, Heini PF, Alini M, Anderson SE, Ito K. 2004 young investigator award winner: vertebral endplate marrow contact channel occlusions and intervertebral disc degeneration. *Spine*. 2005;*30*(2):167-173.
20. Feng C, Liu H, Yang M, Zhang Y, Huang B, Zhou Y. Disc cell senescence in intervertebral disc degeneration: causes and molecular pathways. *Cell Cycle*. 2016;*15*(13):1674-1684.
21. Le Maitre CL, Freemont AJ, Hoyland JA. Accelerated cellular senescence in degenerate intervertebral discs: a possible role in the pathogenesis of intervertebral disc degeneration. *Arthritis Res Ther*. 2007;*9*(3):R45.
22. Rutges J, Duit R, Kummer J, et al. A validated new histological classification for intervertebral disc degeneration. *Osteoarthr Cartil*. 2013;*21*(12):2039-2047.
23. Johnson WE, Caterson B, Eisenstein SM, Hynds DL, Snow DM, Roberts S. Human intervertebral disc aggrecan inhibits nerve growth in vitro. *Arthritis Rheum*. 2002;*46*(10):2658-2664.
24. Purmessur D, Cornejo MC, Cho SK, et al. Intact glycosaminoglycans from intervertebral disc-derived notochordal cell-conditioned media inhibit neurite growth while maintaining neuronal cell viability. *Spine J*. 2015;*15*(5):1060-1069.
25. Freemont A, Peacock T, Goupille P, Hoyland J, O'Brien J, Jayson M. Nerve ingrowth into diseased intervertebral disc in chronic back pain. *The Lancet*. 1997;*350*(9072):178-181.
26. Peng B, Wu W, Hou S, Li P, Zhang C, Yang Y. The pathogenesis of discogenic low back pain. *J Bone Joint Surg Br*. 2005;*87*(1):62-67.
27. García-Cosamalón J, Del Valle ME, Calavia MG, et al. Intervertebral disc, sensory nerves and neurotrophins: who is who in discogenic pain? *J Anat*. 2010;*217*(1):1-15.
28. Abe Y, Akeda K, An HS, et al. Proinflammatory cytokines stimulate the expression of nerve growth factor by human intervertebral disc cells. *Spine*. 2007;*32*(6):635-642.
29. Purmessur D, Freemont AJ, Hoyland JA. Expression and regulation of neurotrophins in the nondegenerate and degenerate human intervertebral disc. *Arthritis Res Ther*. 2008;*10*(4):1-9.
30. Zhang J-M, An J. Cytokines, inflammation and pain. *Int Anesthesiol Clin*. 2007;*45*(2):27-37.
31. Kimmel H, Rahn M, Gilbert TW. The clinical effectiveness in wound healing with extracellular matrix derived from porcine urinary bladder matrix: a case series on severe chronic wounds. *J Am Col Certif Wound Spec*. 2010;*2*(3):55-59.
32. Naderi N, Joji N, Kang NV. Use of dCELL (Decellularized Human Dermis) in Repair of Urethrocutaneous Fistulas or Glans Dehiscence. *Plast Reconst Surg Glob Open*. 2020;*8*(10):e3152.
33. Bondioli E, Purpura V, Orlandi C, et al. The use of an acellular matrix derived from human dermis for the treatment of full-thickness skin wounds. *Cell Tissue Bank*. 2019;*20*(2):183-192.
34. Franklin ME, Trevino JM, Portillo G, Vela I, Glass JL, González JJ. The use of porcine small intestinal submucosa as a prosthetic material for laparoscopic hernia repair in infected and potentially contaminated fields: long-term follow-up. *Surg Endosc*. 2008;*22*(9):1941-1946.
35. Oelschlager BK, Pellegrini CA, Hunter J, et al. Biologic prosthesis reduces recurrence after laparoscopic paraesophageal hernia repair: a multicenter, prospective, randomized trial. *Ann Surg*. 2006;*244*(4):481-490.
36. Liu Y, Cao Z, Yang H, Shen Y, Chen J. Porcine small intestinal submucosa mesh to treat inguinal hernia in young adults using laparoscopic inguinal hernia repair: a retrospective controlled study. *Surg Laparosc Endosc Percutan Tech*. 2020;*30*(4):367-370.
37. Crapo PM, Gilbert TW, Badylak SF. An overview of tissue and whole organ decellularization processes. *Biomaterials*. 2011;*32*(12):3233-3243.
38. Mercuri JJ, Gill SS, Simionescu DT. Novel tissue-derived biomimetic scaffold for regenerating the human nucleus pulposus. *J Biomed Mater Res A*. 2011;*96*(2):422-435.
39. Mercuri JJ, Patnaik S, Dion G, Gill SS, Liao J, Simionescu DT. Regenerative potential of decellularized porcine nucleus pulposus hydrogel scaffolds: stem cell differentiation, matrix remodeling, and biocompatibility studies. *Tissue Eng Part A*. 2013;*19*(7–8):952-966.
40. Hensley A, Rames J, Casler V, et al. Decellularization and characterization of a whole intervertebral disk xenograft scaffold. *J Biomed Mater Res A*. 2018;*106*(9):2412-2423.

41. Chan LK, Leung VY, Tam V, Lu WW, Sze K, Cheung KM. Decellularized bovine intervertebral disc as a natural scaffold for xenogenic cell studies. *Acta Biomater*. 2013;*9*(2):5262-5272.
42. Zhou X, Wang J, Huang X, et al. Injectable decellularized nucleus pulposus-based cell delivery system for differentiation of adipose-derived stem cells and nucleus pulposus regeneration. *Acta Biomater*. 2018;*81*:115-128.
43. Xu J, Liu S, Wang S, et al. Decellularised nucleus pulposus as a potential biologic scaffold for disc tissue engineering. *Mater Sci Eng C*. 2019;*99*:1213-1225.
44. Yu L, Sun Z-J, Tan Q-C, et al. Thermosensitive injectable decellularized nucleus pulposus hydrogel as an ideal biomaterial for nucleus pulposus regeneration. *J Biomater Appl*. 2020;*35*:182-192.
45. Romereim SM, Johnston CA, Redwine AL, Wachs RA. Development of an in vitro intervertebral disc innervation model to screen neuroinhibitory biomaterials. *J Orthop Res*. 2020;*38*(5):1016-1026.
46. Ignat'eva NY, Danilov N, Averkiev S, Obrezkova M, Lunin V. Determination of hydroxyproline in tissues and the evaluation of the collagen content of the tissues. *J Anal Chem*. 2007;*62*(1):51-57.
47. ISO 10993-5, Biological evaluation of medical devices—part 5: tests for in vitro cytotoxicity, 2009, p. 34.
48. ISO 10993-12, Biological evaluation of medical devices—part 12: sample preparation and reference materials, 2012, p. 21.
49. Galili U, Shohet S, Kobrin E, Stults C, Macher B. Man, apes, and Old World monkeys differ from other mammals in the expression of alpha-galactosyl epitopes on nucleated cells. *J Biol Chem*. 1988;*263*(33):17755-17762.
50. Freytes DO, Martin J, Velankar SS, Lee AS, Badylak SF. Preparation and rheological characterization of a gel form of the porcine urinary bladder matrix. *Biomaterials*. 2008;*29*(11):1630-1637.
51. Johnson TD, Lin SY, Christman KL. Tailoring material properties of a nanofibrous extracellular matrix derived hydrogel. *Nanotechnology*. 2011;*22*(49):494015.
52. Li Y, Douglas EP. Effects of various salts on structural polymorphism of reconstituted type I collagen fibrils. *Colloids Surf B Biointerfaces*. 2013;*112*:42-50.
53. Morozova S, Muthukumar M. Electrostatic effects in collagen fibril formation. *J Chem Phys*. 2018;*149*(16):163333.
54. Iatridis JC, Setton LA, Weidenbaum M, Mow VC. Alterations in the mechanical behavior of the human lumbar nucleus pulposus with degeneration and aging. *J Orthop Res*. 1997;*15*(2):318-322.
55. Iatridis JC, Setton LA, Weidenbaum M, Mow VC. The viscoelastic behavior of the non-degenerate human lumbar nucleus pulposus in shear. *J Biomech*. 1997;*30*(10):1005-1013.
56. Brown JM, Xia J, Zhuang B, et al. A sulfated carbohydrate epitope inhibits axon regeneration after injury. *Proc Natl Acad Sci*. 2012;*109*(13):4768-4773.
57. Fornaro M, Giovannelli A, Foggetti A, et al. Role of neurotrophic factors in enhancing linear axonal growth of ganglionic sensory neurons in vitro. *Neural Regen Res*. 2020;*15*(9):1732-1739.
58. Sholl DA. Dendritic organization in the neurons of the visual and motor cortices of the cat. *J Anat*. 1953;*87*(Pt 4):387.
59. Nerurkar NL, Elliott DM, Mauck RL. Mechanical design criteria for intervertebral disc tissue engineering. *J Biomech*. 2010;*43*(6):1017-1030.
60. Franze K. The mechanical control of nervous system development. *Development*. 2013;*140*(15):3069-3077.
61. Thomas AM, Kubilius MB, Holland SJ, et al. Channel density and porosity of degradable bridging scaffolds on axon growth after spinal injury. *Biomaterials*. 2013;*34*(9):2213-2220.
62. Tolofari SK, Richardson SM, Freemont AJ, Hoyland JA. Expression of semaphorin 3A and its receptors in the human intervertebral disc: potential role in regulating neural ingrowth in the degenerate intervertebral disc. *Arthritis Res Ther*. 2010;*12*(1):1-11.
63. Nakazawa KR, Walter BA, Laudier DM, et al. Accumulation and localization of macrophage phenotypes with human intervertebral disc degeneration. *Spine J*. 2018;*18*(2):343-356.
64. Antoniou J, Steffen T, Nelson F, et al. The human lumbar intervertebral disc: evidence for changes in the biosynthesis and denaturation of the extracellular matrix with growth, maturation, ageing, and degeneration. *J Clin Invest*. 1996;*98*(4):996-1003.
65. Perie DS, Maclean JJ, Owen JP, Iatridis JC. Correlating material properties with tissue composition in enzymatically digested bovine annulus fibrosus and nucleus pulposus tissue. *Ann Biomed Eng*. 2006;*34*(5):769-777.
66. Johannessen W, Elliott DM. Effects of degeneration on the biphasic material properties of human nucleus pulposus in confined compression. *Spine*. 2005;*30*(24):E724-E729.
67. O'Neill JD, Anfang R, Anandappa A, et al. Decellularization of human and porcine lung tissues for pulmonary tissue engineering. *Ann Thorac Surg*. 2013;*96*(3):1046-1056.
68. Lau CS, Hassanbhai A, Wen F, et al. Evaluation of decellularized tilapia skin as a tissue engineering scaffold. *J Tissue Eng Regen Med*. 2019;*13*(10):1779-1791.

How to cite this article: Piening, L. M., Lillyman, D. J., Lee, F. S., Lozano, A. M., Miles, J. R., & Wachs, R. A. (2022). Injectable decellularized nucleus pulposus tissue exhibits neuroinhibitory properties. *JOR Spine*, *5*(1), e1187. https://doi.org/10.1002/jsp2.1187